Combined IVIM and DTI for simultaneous assessment of diffusion and flow anisotropy of the kidney

Mike Notohamiprodjo[1,2], Hersh Chandarana[3], Artem Mikheev[2], Jose Garcia Raya[2], John Grinstead[4], Thorsten Feiweier[4], Henry Rusinek[3], Vivian S Lee[3,5], and Eric E Sigmund[2]

[1]*Department of Clinical Radiology, University Hospitals Munich, Munich, Bavaria, Germany,* [2]*Center for Biomedical Imaging, NYU Langone Medical Center, New York City, NY, United States,* [3]*Department of Radiology, NYU Langone Medical Center,* [4]*Siemens Healthcare,* [5]*University of Utah Health Care*

Purpose: Diffusion weighted imaging characterizes water motion on a molecular level and provides information about renal microstructure and function. One variant, intravoxel incoherent motion (IVIM), distinguishes tubular/vascular flow from passive diffusion through collecting data over a range of diffusion weightings (or b-values) (1, 2). Another, diffusion tensor Imaging (DTI), is sensitive to direction of restriction (anisotropy) to diffusion through analysis of multiple diffusion-sensitizing directions, and demonstrates clear anisotropy in the renal medulla (2, 3). However, the biophysical underpinning of this anisotropy remains unproven, particularly regarding the roles of (a) structural restrictions of tubules and collecting ducts and (b) active flow in oriented tubular or vascular structures (5). Resolving this ambiguity requires a more comprehensive acquisition and analysis approach. In the present study, we used a combined IVIM-DTI methodology to distinguish structural from flow effects on renal tissue anisotropy, which may be useful in the evaluation of diabetic nephropathy or allograft rejection.

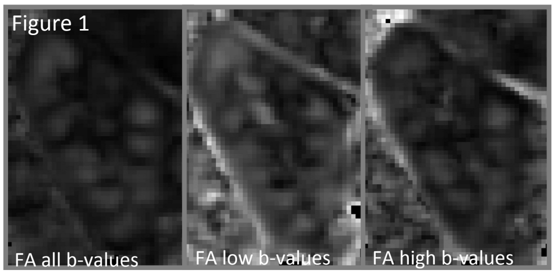

Material and Methods: Eight healthy volunteers were examined using a clinical 3T-scanner (VERIO, Siemens Healthcare). IVIM-DTI was acquired during free-breathing using a twice-refocused spin echo Echo-Planar-Imaging sequence with extra fat suppression and nonlinear phase correction and with following parameters: TR 2600ms; TE 79ms; 2 averages; 20 diffusion directions; b-values 0, 10, 30, 50, 80, 120, 200, 400, 600, 800 s/mm^2; slice thickness 6mm. Retrospective 2D affine coregistration of all images to mitigate respiratory motion artifact was performed with FireVoxel software (6). IVIM-DTI analysis of the renal cortex and medulla was performed using custom code (IgorPro 6, Wavemetrics, Inc.). Several variants of analysis were performed to investigate the interplay of flow and anisotropy. First, mean diffusivity (MD) and fractional anisotropy (FA) from conventional DTI analysis was measured for the low (b= 0-200), high (b=400-800) and full (b=0-800) b-value range. Second, for each acquired direction, IVIM-parameters perfusion fraction f_P, pseudo-diffusivity D_p and tissue diffusivity D_t were calculated with a *segmented* voxelwise analysis: (1) D_t was determined from a monoexponential fit using values for b > 200 s/mm^2; (2) The zero intercept from step (1) is used along with the b=0 signal to determine f_P. (3) D_P was calculated from a biexponential fit with constrained D_t and f_p. Maps of mean and standard deviation (i.e. directional variance) of D_t, f_p, and D_p over all directions were generated. The global anisotropies of D_t and f_P were visualized as follows: Regions of interest (ROIs) were manually drawn segmenting cortex and medulla on all slices. The primary diffusion eigenvector $\hat{e}_1$ in each voxel was measured from a diffusion tensor analysis of the measured D_t values. Then, the D_t or f_p values from all ROI voxels in 20 directions (total >1000 points/subject) were plotted as a function of the relative angle between the diffusion direction $\hat{g}$ and $\hat{e}_1$ (i.e. a "peanut plot") (3). Finally, the mean and standard deviation of data within angular bins of the ROI scatter plot were calculated for an averaged representation (6). Effective FA values reflecting D_t and f_p anisotropy were estimated from the 0° (axial, along $\hat{e}_1$) and 90° (radial, perpendicular to $\hat{e}_1$) values of the averaged angular distribution. Statistical analysis was performed with paired t-tests to compare cortical and medullary values of the parameters described above (*=p<0.05).

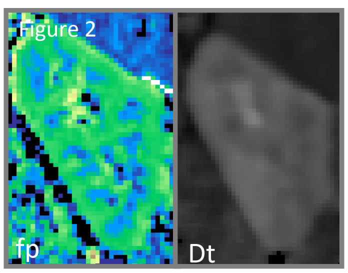

	MD		FA	
	Cortex	**Medulla**	**Cortex**	**Medulla**
0<b<800	2.1±0.1	2.1±0.1	0.14±0.05	0.30±0.13*
0<b<200	3.3±0.5	2.9±0.4	0.25±0.09	0.40±0.10*
400<b<800	1.8±0.1	1.8±0.1	0.22±0.08	0.27±0.07*

Table 1: Kidney DTI parameters as a function of b-value range. * indicates statistiscal significant Ctx/Med diff

Results: FA of the medulla was significantly higher than of the cortex for all 3 b-value-regimes, however the corticomedullary difference is smaller for the high b-value range (**Table 1** and **Figure 1**). **Table 2** summarizes data from the combined IVIM-DTI analysis for all 8 volunteers in this study. A significantly higher f_p and higher D_t was determined for the cortex than for the medulla (**Figure 2**) Both f_p and D_t showed a significantly higher directional variance σ in medulla than cortex (**Table 2**). The polar plot analysis depicts nearly isotropic f_P and D_t in the cortex and anisotropy for both D_t and f_p parameters in the medulla (**Figure 3**).

	Cortex	**Medulla**
$\langle D_t \rangle$	2.34±0.14	2.28±0.21
$\sigma(D_t)$	0.16±0.02	0.32±0.05*
$D_{t\ axial}$	2.64±0.20	2.95±0.34
$D_{t\ radial}$	2.18±0.19	1.88±0.20
FA(D_t)	0.11±0.02	0.28±0.03*
$\langle f_p \rangle$	26.6±6.1	14.1±4.5*
$\sigma(f_p)$	6.7±3.2	12.2±4.8*
$f_{p\ axial}$	25.2±2.2	29.1±3.4
$f_{p\ radial}$	21.5±2.6	15.5±2.2
FA(f_p)	0.12±0.02	0.31±0.05*

Table 2: Combined IVIM-DTI analysis. Mean and directional variance (σ) values, along with axial, radial, and FA values derived from the angular scatterplot (in blue) are shown for D_t and f_p.

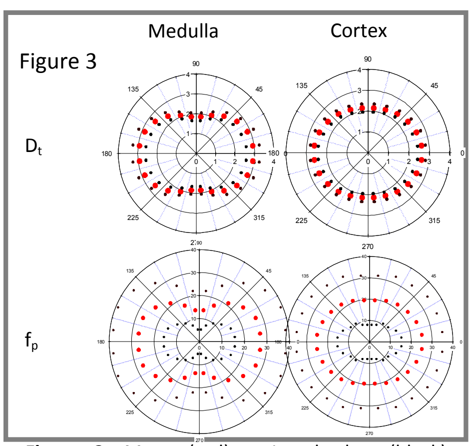

Figure 3: Mean (red) ± 1 std. dev. (black) averaged angular distribution of IVIM parameters D_t and f_p in tissue ROI voxels referenced to primary D_t eigenvectors $\hat{e}_1$.D_t and f_p. These results indicate strong anisotropy in the medulla.

Conclusions: Our data suggest that a combined IVIM-DTI protocol is feasible during free-breathing, when combined with co-registration. The combined IVIM-DTI approach also provides several compelling findings. First, we observe significantly higher f_p of the cortex than medulla, in distinction from previous studies finding comparable f_p in both tissues. Second, higher medullary FA at the low b-value range and high directional variance of medullary f_p suggest anisotropy of the perfusion fraction. Similarly, both flow and diffusion appear to contribute to the diffusion anisotropy of the renal medulla. Future application of this novel method may be useful in separating decreased tubular flow from irreversible structural tubular damage, e.g. in diabetic nephropathy.

References: (1) Le Bihan, Radiology. 1986 Nov;161(2):401-7; (2) Thoeny et al.; Radiology. 2006 Dec;241(3):812-21. (3) Notohamiprodjo et al.; Invest Radiol. 2010 May;45(5):245-54 (4) Ries M et al.; J Magn Reson Imaging. 2001 Jul;14(1):42-9. (5) Sigmund EE et al;; ISMRM 2011 (6) Jones DK and Basser PJ Magn Reson Med. 2004 Nov;52(5):979-93 (6) Patel J et al.; J Magn Reson Imagin. 2010 31:589-600.